NANO · MICRO small
www.small-journal.com

Therapeutic Gene Silencing Using Targeted Lipid Nanoparticles in Metastatic Ovarian Cancer

*Manu Smriti Singh, Srinivas Ramishetti, Dalit Landesman-Milo, Meir Goldsmith, Sushmita Chatterjee, Ramesh Palakuri, and Dan Peer**

Ovarian cancer is an aggressive tumor owing to its ability to metastasize from stage II onward. Herein, lipid nanoparticles (LNPs) that encapsulate combination of small interfering RNAs (siRNAs), polo-like kinase-1 (PLK1), and eukaryotic translation-initiation factor 3c (eIF3c), to target different cellular pathways essential for ovarian cancer progression are generated. The LNPs are further modified with hyaluronan (tNPs) to target cluster of differentiation 44 (CD44) expressing cells. Interestingly, hyaluronan-coated LNPs (tNPs) prolong functional activity and reduce growth kinetics of spheroids in in vitro assay as compared to uncoated LNPs (uNPs) due to ≈1500-fold higher expression of CD44. Treatment of 2D and 3D cultured ovarian cancer cells with LNPs encapsulating both siRNAs result in 85% cell death and robust target gene silencing. In advanced orthotopic ovarian cancer model, intraperitoneal administration of LNPs demonstrates CD44 specific tumor targeting of tNPs compared to uNPs and robust gene silencing in tissues involved in ovarian cancer pathophysiology. At very low siRNA dose, enhanced overall survival of 60% for tNPs treated mice is observed compared to 10% and 20% for single siRNA-, eIF3c-tNP, and PLK1-tNP treatment groups, respectively. Overall, LNPs represent promising platform in the treatment of advanced ovarian cancer by improving median- and overall-survival.

1. Introduction

Ovarian cancer is the leading cause of gynaecological mortality worldwide. 80% of the ovarian cancer patients are diagnosed at an advanced stage (III and IV) when the 5-year survival is only 29% as compared to an early diagnosis when the 5-year survival is 92%.[1] Advanced ovarian cancer is marked by presence of tumor metastasis in omentum, peritoneal wall, diaphragm, gastrointestinal tract, and liver via transcoelomic route. In most cases, this is accompanied by fluid accumulation in peritoneal cavity also called ascites,[2] which is comprised of clusters of cancer cells with or without fibroblasts, mesothelial cells, adipocytes, and endothelial cells. Such advanced stage patients are treated with neoadjuvant chemotherapy with delayed or interval debulking surgery. Chemotherapy, however, is often associated with development of chemoresistance with a chance of relapse as high as 70% within 18 months.[2] Promising results from randomized clinical trials of ovarian cancer patients by folate receptor inhibitors, PARP inhibitors and anti-angiogenic therapies have led to their approval and/or perusal in clinical settings.[3] Besides conventional surgical and chemotherapy intervention, focus is now shifting to molecular therapies for targeted effects.

RNA interference (RNAi), the cellular mechanism which regulates protein expression, holds a great potential as a molecular cancer therapy strategy. Exogenous introduction of short sequences of double-stranded RNA, which are further processed into small interfering RNA (siRNA) can trigger nucleolytic degradation of target mRNA in cytoplasm in a sequence-specific manner. The physiological challenges such as immunogenicity, renal

Dr. M. S. Singh, Dr. S. Ramishetti, Dr. D. Landesman-Milo, Dr. M. Goldsmith, Dr. S. Chatterjee, Dr. R. Palakuri, Prof. D. Peer
Laboratory of Precision NanoMedicine
Tel Aviv University
Tel Aviv 69978, Israel
E-mail: peer@tauex.tau.ac.il

Dr. M. S. Singh, Dr. S. Ramishetti, Dr. D. Landesman-Milo, Dr. M. Goldsmith, Dr. S. Chatterjee, Dr. R. Palakuri, Prof. D. Peer
School of Molecular Cell Biology & Biotechnology
George S. Wise Faculty of Life Sciences
Tel Aviv University
Tel Aviv 69978, Israel

The ORCID identification number(s) for the author(s) of this article can be found under https://doi.org/10.1002/smll.202100287.

DOI: 10.1002/smll.202100287

Dr. M. S. Singh, Dr. S. Ramishetti, Dr. D. Landesman-Milo, Dr. M. Goldsmith, Dr. S. Chatterjee, Dr. R. Palakuri, Prof. D. Peer
Department of Materials Sciences & Engineering
Iby and Aladar Fleischman Faculty of Engineering
Tel Aviv University
Tel Aviv 69978, Israel

Dr. M. S. Singh, Dr. S. Ramishetti, Dr. D. Landesman-Milo, M. Goldsmith, Dr. S. Chatterjee, Dr. R. Palakuri, Prof. D. Peer
Center for Nanoscience and Nanotechnology
Tel Aviv University
Tel Aviv 69978, Israel

Dr. M. S. Singh, Dr. S. Ramishetti, Dr. D. Landesman-Milo, Dr. M. Goldsmith, Dr. S. Chatterjee, R. Palakuri, Prof. D. Peer
Cancer Biology Research Center
Tel Aviv University
Tel Aviv 69978, Israel

clearance, serum degradation, and cellular uptake hindered the use of negatively charged naked siRNA.[4] Non-viral gene therapy is a promising platform for nucleic acid delivery, among them lipid nanoparticles (LNPs) are the most advanced technology for nucleic acid delivery.[5,6] Foremost, is the recently FDA approved ONPATTRO, LNP-siRNA for the treatment of liver disease transthyretin-mediated amyloidosis.[7]

Polo-like kinase-1 (PLK1) plays an important role in malignant transformation by triggering early G2/M transition during the cell cycle.[8] Downregulation of PLK1 will arrest the cell cycle leading ultimately to cell death. LNP-siPLK1 formulation (TKM-080301) completed phase I/II trial for neuroendocrine and adrenocortical tumor (NCT01262235) and hepatocellular carcinoma (NCT0219878).

Aberration of the protein translation machinery established as a hallmark of neoplasia is being explored as potential therapeutic target modality for cancer.[9] Eukaryotic translation-initiation factor 3C (eIF3c), a core subunit of the eukaryotic translation initiation complex is a crucial factor for translation initiation via polysome run off eventually leading to cell death, as previously reported from our laboratory.[10] eIF3c is shown to drive tumorigenesis through mTOR pathway in breast cancer,[11] promote angiogenesis and tumorigenesis in hepatocellular carcinoma[12] and facilitate proliferation in glioma[13] highlighting its clinical relevance in cancer treatment.

The major problem in treating cancer patients with synthetic nucleic acid-based drugs is lack of localized intracellular delivery of nucleic acid therapeutics to tumor cells. Enhanced permeability and retention effect (EPR effect) facilitates nanoparticles to enter tumor site when the tumor is surrounded by disorganized leaky blood vessels. However, lack of leaky blood vessels in many tumors such as pancreatic, ovarian cancer, and metastasized tumors commands bypassing EPR effect and opting for local delivery (intraperitoneal route) instead of systemic delivery.[14] Additionally, suitable ligands can direct the RNAi-nanoparticles to tumor sites. Cluster of differentiation 44 (CD44), a transmembrane glycoprotein plays an important role in cell-cell interaction overexpressed in many cancer types including ovarian cancer.[15,16] Hyaluronan (HA) is the prime ligand for CD44 receptors. HA coated nanoparticles have shown to taken up efficiently by CD44 expressing tumor cells in many types of cancer.[8,17–19]

Another major problem in treating cancer patients using RNAi therapeutics is transient effect of the RNAi payload. Targeting single pathway may not be enough to kill cancer cells as they always chose alternate pathways to survive. Targeting multiple signaling pathways by pooled siRNA's would be advantageous for better therapeutic outcome.

Toward this end, in the current work, we developed LNPs formulated with siPLK1 and sieIF3c to target both cell cycle and protein translation pathways essential for cancer cell survival. LNPs were further surface modified with HA to facilitate CD44 specific internalization into cancer cells. We tested the efficacy of LNPs in 2D and spheroid-based 3D cultures of ovarian cancer cells in vitro. Furthermore, we established an orthotopic advanced ovarian cancer model in mice to evaluate the efficiency of LNPs by intraperitoneal administration that enhance the localized delivery of RNAi therapeutics at relatively low doses.

2. Results

2.1. Lipid Nanoparticles Preparation and Physicochemical Characterization

The novel lipid 10, previously shown for efficient RNAi delivery to leukocytes was synthesized in-house.[20] The chemical structures were confirmed by ESI-MS and NMR techniques (Figures S1 and S2, Supporting Information). LNPs were prepared by microfluidic mixture composed of ionizable lipid 10, along with other helper lipids such as cholesterol, DSPC, DMG-PEG. DSPE-PEG-amine was included in order to conjugate the HA on the surface of LNPs by conventional EDC/NHS method (**Figure 1**A).[8] The LNPs were smaller in size (<60 nm in diameter) with low polydispersity index (PDI < 0.1) as measured by DLS (Figure 1B). In support to DLS measurements, transmission electron microscopy results demonstrated uniform distribution and smaller size of LNPs (Figure 1D,E). After HA modification the size of LNPs slightly increased and surface potential dropped as confirmed by DLS (Figure 1C). We also observed clear difference in the surface of LNPs before and after HA modifications (Figure 1D,E-inset).

We first evaluated LNPs prepared with our novel ionizable lipid 10 versus gold standard lipid Dlin-MC3-DMA. Cellular uptake of both formulations were compared using Cy5-NC5-siRNA encapsulated LNPs. We observed enhanced cellular uptake of lipid10-LNPs compared to MC3-LNPs in Ovcar8 cells (Figure S3, Supporting Information). We further evaluated functional activity of siPLK1 encapsulated LNPs (lipid 10 vs MC3). Ovcar8 and NCI-adriamycin resistant (NAR) cells treated with both formulations for 72 h induced cell death (Figure S4, Supporting Information). At higher siRNA amounts both formulations showed similar effect on cell viability, however lipid10-LNPs resulted in significant cell death even at lower siRNA amounts compared to MC3-LNPs.

2.2. Cluster of Differentiation 44 Specific Binding and Therapeutic Activity in 3D Spheroids

Ovcar8 cells form reproducible spheroids in ultralow attachment 96-well plates within 3 days of seeding cells (**Figure 2**A). Our lab previously characterized spheroids and showed Ovcar8-based spheroids grow up to 12 days without reaching plateau in terms of spheroid volume.[21] We first evaluated the CD44 expression in Ovcar8 spheroids. We found a 1500-fold increased expression of CD44 in cells grown as spheroids (3D) in comparison to cells cultured in 2D conditions (Figure 2B). As spheroids are hard to penetrate and transfect, we evaluated our LNP-siRNA formulations on spheroids. LNPs encapsulated single siRNA or combination of siRNAs with HA (tNPs) and without HA (uNPs) on the surface were synthesized. Next, we evaluated the entire panel of uncoated and targeted LNPs encapsulating non-coding- siNC5, sieIF3c, siPLK1, and combination siRNAs (eP) to test the effect of LNPs on spheroid growth kinetics following three treatments on day 0, 4, and 8 at 148 nM total siRNA concentration (Figure 2C). On day 0 Ovcar8 cells were seeded in 96-well plate to form spheroid. The spheroid growth kinetics were monitored for 12 days by

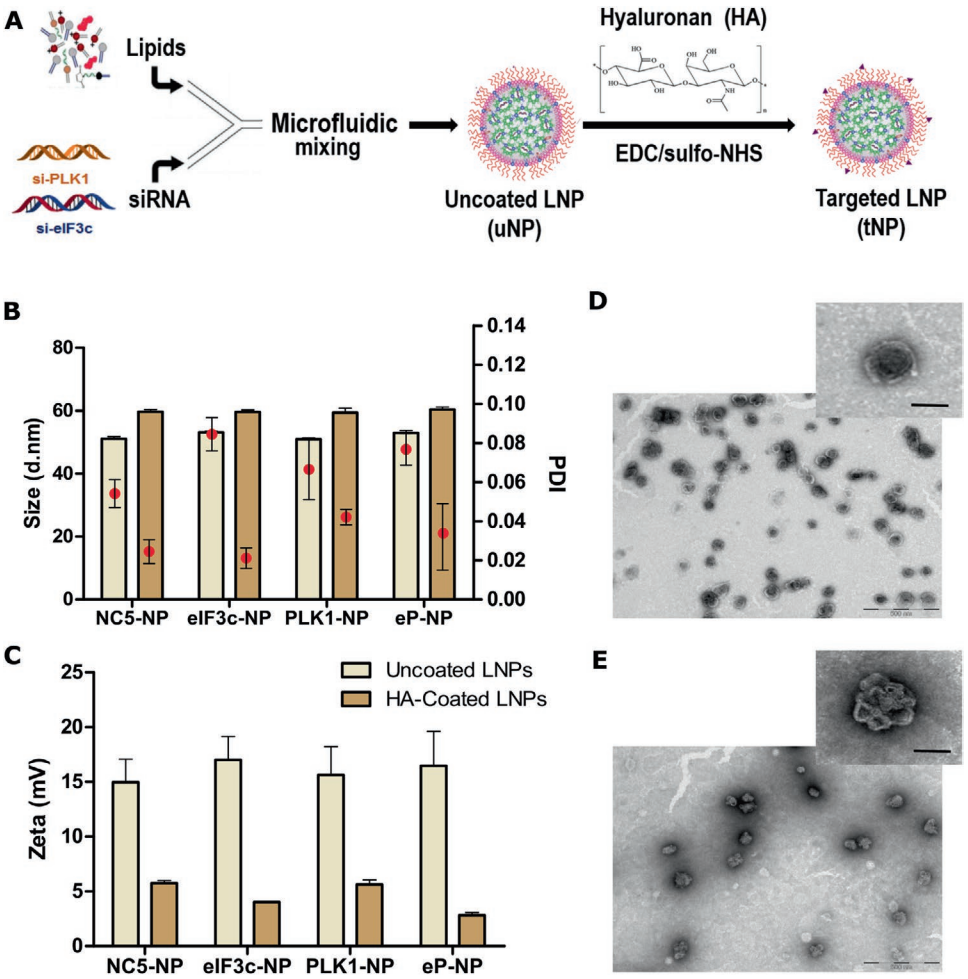

Figure 1. A) Scheme of LNP development. Physicochemical characterization of LNPs: B) Size and polydispersity index (PDI) and C) zeta potential of uncoated and HA-coated LNPs as evaluated using DLS. Transmission electron micrograph (TEM) image of D) uncoated uNP and E) HA-coated targeted tNPs; Scale bar: 500 nm; inset scale bar: 50 nm.

Incucyte in terms of mean fluorescence intensity of mCherry to assess the cell viability. As shown in **Figure 3**D, the spheroid growth is significantly inhibited (≈50%) in eP-tNP treatment group as compared to control groups (untreated and NC5-NP). Overall, the spheroid volume decreased by 46% in comparison to untreated spheroids on day 12 (Figure 2E). Between each group of NC5, eIF3c, PLK1, and eiF3c-PLK1 (eP) combination, the tNPs showed significant percent reduction of spheroid volume than the uNPs. The results demonstrate functional role of hyaluronan coating on tNPs which is directly associated with CD44 expression. Additionally, HA-coated LNP binding was notably observed in 2D cultured Ovcar8 cells at 4 °C for 30 min (Figure S5, Supporting Information). We further treated 3-day spheroids with eP-tNPs (74 nM) for 72 h to evaluate the extent of gene silencing achieved. Interestingly, both PLK1 and eIF3c genes were significantly downregulated (≈80%) in spheroids treated with eP-tNP normalized to either untreated control (Figure S6, Supporting Information) or NC5-NP treated group (Figure 2F). This CD44-mediated uptake of HA-coated particles verified the superior results obtained with tNPs in terms of decline of spheroid growth.

2.3. sieIF3c and siPLK1 Exhibit Strong Functional Activity In Vitro

After confirming CD44 specific uptake of HA coated LNPs in 3D cultures we decided to use HA coated LNPs for further experiments. Next, we evaluated the functional activity of each of the selected siRNA molecules in 2D cultures of Ovcar8. As shown in Figure 3A, Ovcar8 cells treated with HA coated LNPs encapsulated sieIF3c (eIF3c-tNP) led to over 90% gene silencing at both higher and lower doses indicating the efficiency of LNPs to deliver siRNA inside the cells. Next, the effect of eIF3c downregulation on protein synthesis was evaluated. We performed puromycin incorporation assay by inducing premature translation termination in Ovcar8 cells growing as 2D or 3D culture treated with eIF3c-tNP.[22] The cells were lysed and puromycylated proteins detected on western blots using antibody against Puromycin (Figure 3B). Quantitatively, we noted ≈30% and ≈40% lesser puromycin (Figure 3C) in eIF3c-tNP treated 2D and 3D cultures respectively demonstrating the decline in newly translated proteins.

We further evaluated the second gene-PLK1 for its functional characterization. As shown in Figure 3D, efficient

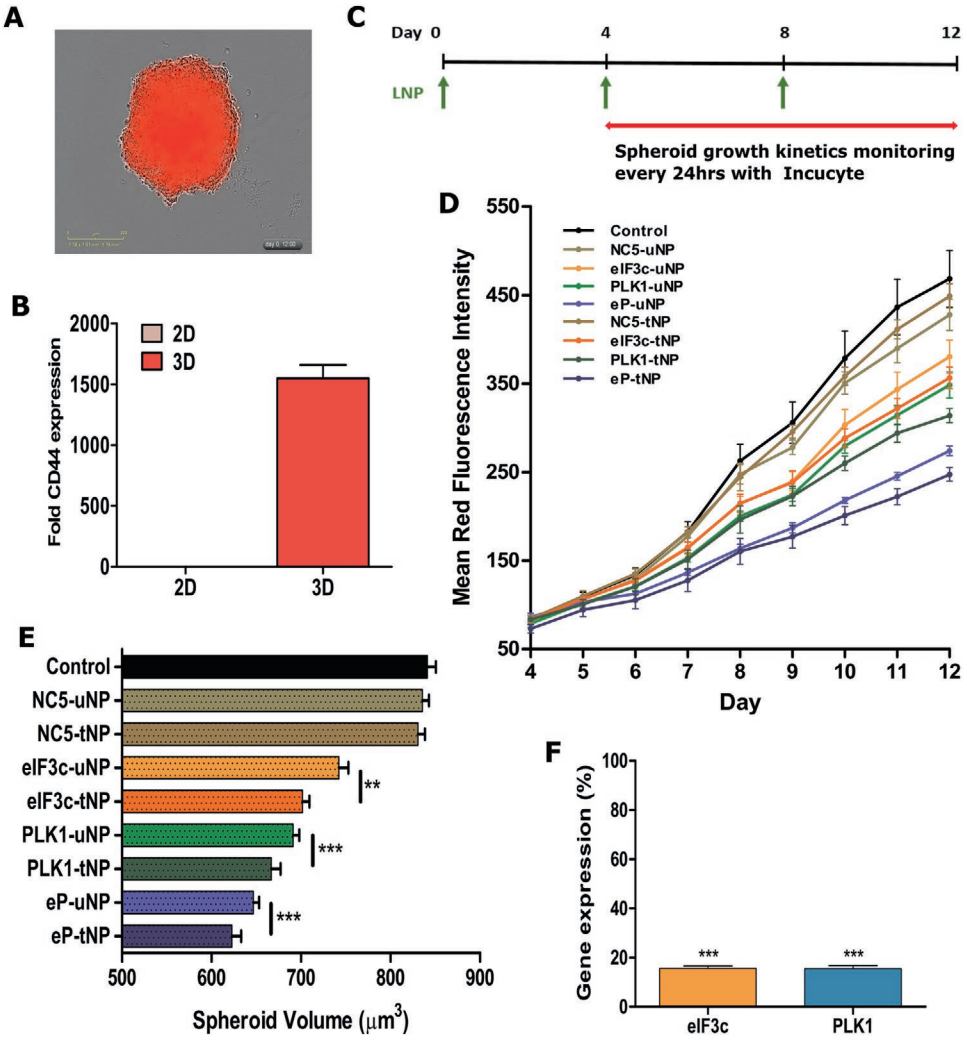

Figure 2. Evaluation of LNPs in single spheroids. A) Image of single spheroid from Ovcar8 on day 3. B) Fold CD44 expression in Ovcar8 cells grown as 2D cell culture and 3D spheroids. GAPDH was used as housekeeping gene. C) Scheme of seeding, treatment of spheroids (148 nM siRNA equivalent LNPs) to monitor spheroid growth kinetics. D) Spheroid growth kinetics measured as mean red fluorescence of mCherry-labelled viable cells over 12 days of spheroid culture. E) Spheroid volume on day 12. F) Silencing of both genes in spheroids treated with combination eP-tNP (74 nM) for 72 h showing robust silencing of over 80% normalized to gene expression in NC5-NP treated spheroid. Two-way ANOVA followed by Bonferroni post test ($n = 3$); ***$p < 0.001$.

gene silencing (80–90%) was observed in a dose-dependent manner in Ovcar8 cells treated with siPLK1 encapsulated HA-LNPs (PLK1-tNP). Next, we evaluated the effect of PLK1 inhibition on functional activity of cell cycle arrest and apoptosis.[8,23] Cell cycle profile assayed 24 h post LNP treatment, showed 2% of the cell population was arrested at G0/G1 phase in PLK1-tNP treatment group in contrast to ≈49% cells in untreated group (Figure 3E,F). The fraction of G2/M phase increased from 26% to 85% cells in siPLK1-treated cells demonstrating strong anti-proliferative activity of PLK1-tNPs. As shown in Figure 2G, PLK1-tNP treatment led to ≈20% of the cells found in early apoptosis and over ≈40% dead cells (Figure S7, Supporting Information) indicating loss of cell viability due to the strong anti-proliferative activity of PLK1 on cancer cells.

After the evaluation of both PLK1 and eIF3c genes functional activity, we next evaluated the efficiency of HA-LNPs encapsulating both siRNAs- eIF3c and PLK1 on gene inhibition and cell survival. We observed significant gene inhibitions of both PLK1 and eIF3c genes in cells treated with eP-tNP (Figure 3H).

Next, Ovcar8 (Figure 3I and Figure S8, Supporting Information) and NAR cells (Figure S9, Supporting Information) were treated with LNPs encapsulating either sieIF3c or siPLK1 or both at different siRNA concentrations and different time points to assess the cell death. It is important to note that the total amount of siRNA in eP-tNP is same as individual NPs. At 72 h time point the EC50 values for cytotoxicity are <18 nM for eP-tNP and PLK1-tNP compared to 74 nM for eIF3c-tNP. Additionally, the EC50 values are lower even after 96 h for eP-tNP and PLK1-tNP compared to eIF3c-tNPs (Figure S8, Supporting Information). Lower EC50 values for eP-NP attributed to targeting multi signaling pathways by both siPLK1 and sieIF3c that affect cell viability significantly at half of the siRNA amounts present in either PLK1-tNP or eIF3c-tNP.

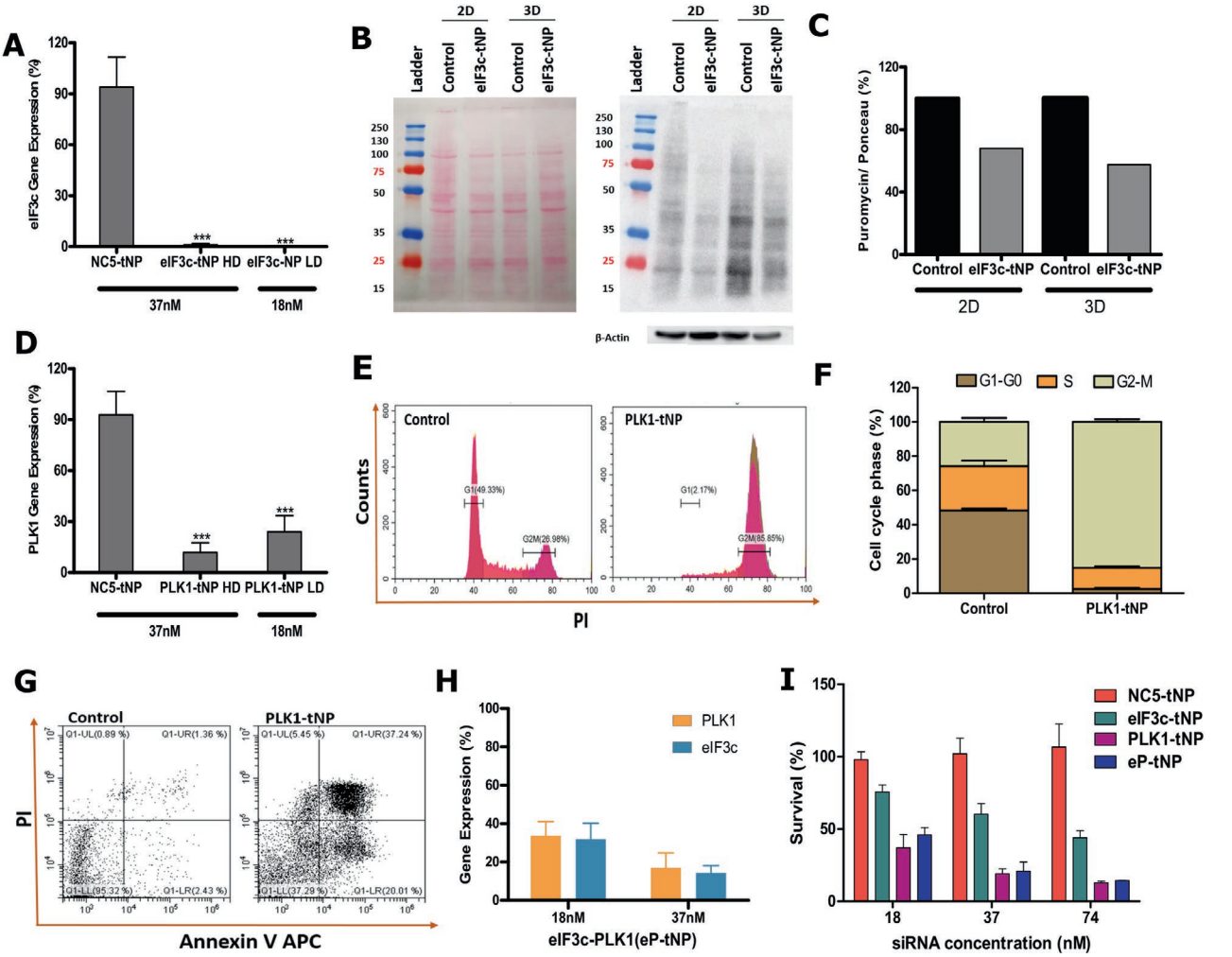

Figure 3. A) Ovcar8 cells were treated with eIF3c-tNP or D) PLK1-tNP for 72 h. The treated cells showed robust gene silencing of both eIF3c and PLK1 as normalized against NC5-tNP group. B) After 72 h treatment with eIF3c-tNP (74 nM), cells were treated with puromycin (2.5μg mL^{-1}) for 5 min. Equal amounts of protein extract were analyzed by western blotting with either: Left-ponceau S staining showing total protein levels and right-anti-uromycin antibody. C) Puromycin/ponceau S signal to quantify newly synthesized polypeptides. E) Cell cycle progression from G2 to M phase in Ovcar8 cells-untreated (left) and PLK1-tNP (37 nM) treated (right) for 24 h; F) Percent cells in each cell cycle phase. G) Annexin V/PI staining of cells untreated (control) and PLK1-tNP (37 nM) treated for 48 h. H) Gene expression (%) of PLK1 and eIF3c in cells treated with combination eIF3c+PLK1 NP (eP-tNP) treated for 72 h. GAPDH was used as endogenous control and the results are normalized to NC5-NP treatment group. Robust and dose-dependent silencing was observed with combination siRNAs. I) Ovcar8 cells were treated with 18, 37, and 74 nM equivalent siRNA concentration for 72 h. eP-tNP treatment contained half equivalent concentration of both eIF3c and PLK1 but total siRNA concentration (nM) was same. Cell viability was evaluated with XTT assay and dose dependent cell death was observed following LNP treatment containing target siRNA. (***$p < 0.05$; One way ANOVA followed by Dunnett's test) ($n = 3$).

2.4. Hyaluron Coated Lipid Nanoparticles Show Enhanced Binding and Internalization in to Tumor Cells In Vivo

The orthotopic ovarian cancer mice model with Ovcar8 cells grows around peritoneal cavity eventually forming ascites and resembles clinical pathology closely.[23,24] We evaluated if there is any advantage of HA-coating LNPs in terms of LNP binding and silencing in vivo. siCy5 labelled LNPs (either uNPs or tNPs) were injected intraperitoneally in to tumor bearing mice (**Figure 4**A,B). Mice were sacrificed and imaged using Maestro in vivo fluorescence imaging system (Cri MA, USA). As shown in Figure 4C, overlapping of Cy5 fluorescence with mCherry signal in mice treated with HA coated LNPs (right) compared to uncoated LNPs (uNPs) (left). Quantitative data in Figure 4D, demonstrating clearly that HA-LNPs are binding or/and penetrating more in tumor cells through CD44 receptors expressed on tumor cells, whereas low or negligible amount of LNPs accumulated in to tumor cells. To support this data, we further tested siPLK1 encapsulated LNPs (either uNPs or tNPs) as proof-of-concept before starting in vivo therapeutic efficacy study on large scale. As shown in Figure 4E, significant amount of PLK1 gene downregulation observed in all major organs involved in ovarian cancer pathophysiology-ovaries, omentum, and ascites compared to uNPs. HA-LNPs. This together with our previous results in glioblastoma model[8] where HA-coated LNPs provided overall benefit over non-coated LNPs in enhanced targeting to cancer cells, led us to do all further in vivo studies using only HA-coated LNPs.

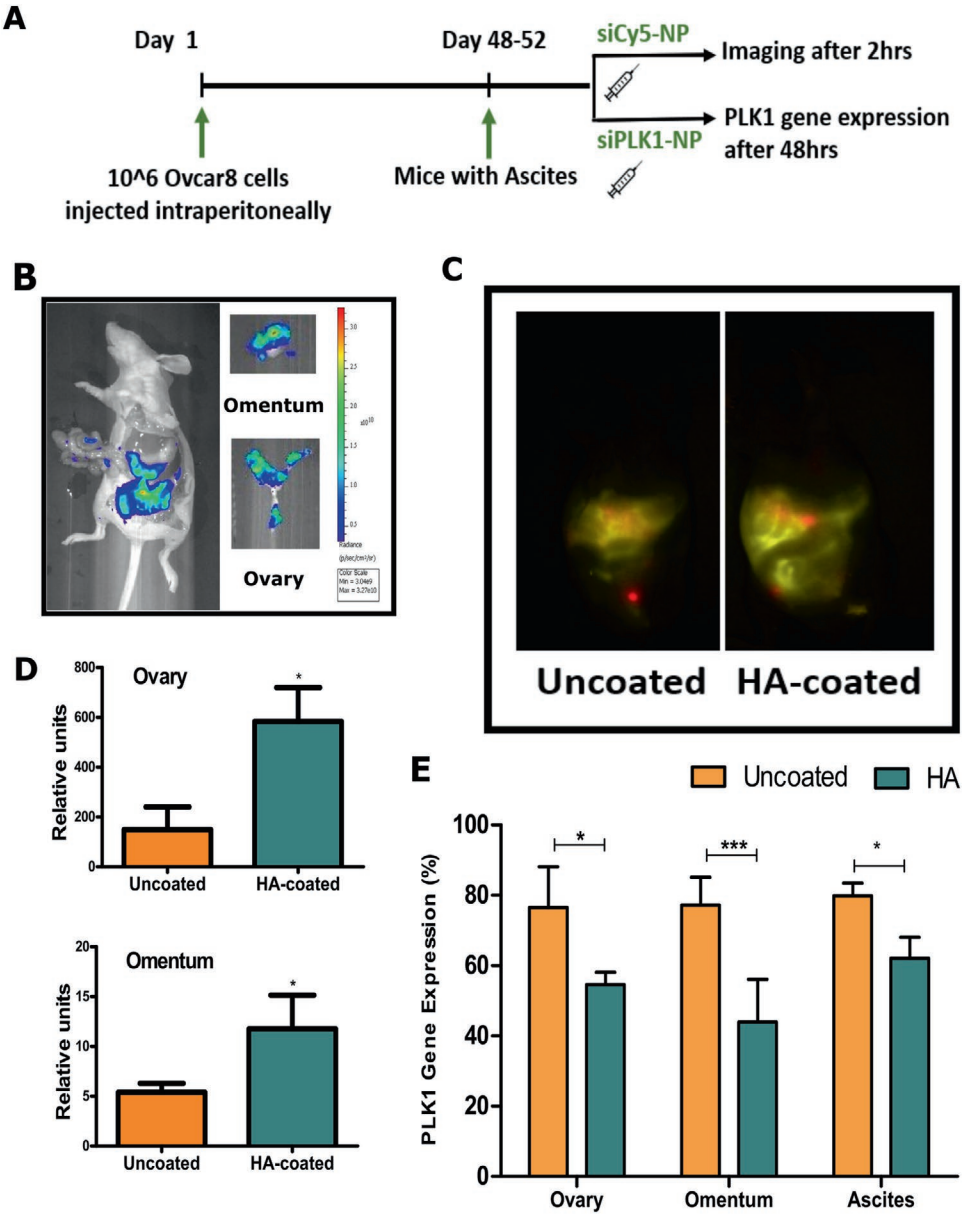

Figure 4. A) Scheme of experiment. B) Representative mice showing presence of ovarian tumor across peritoneal cavity- intestine, omentum, and ovary. C) Mice injected with Cy5-NP and imaged after 2 h to evaluate LNP distribution in mCherry labelled tumors. D) Ovary and omentum were harvested and Cy5 intensity normalized for mCherry signal were calculated ($n = 4$). E) Mice were injected 1 mg kg^{-1} siPLK1-LNPs (with/without HA-coating) intraperitoneally on day 48. Mice were euthanized 48 h post LNP injection. Ovary and omentum were harvested and analyzed for % gene expression of PLK1 mRNA levels to evaluate targeting efficacy of two groups of uncoated and HA-coated LNPs; two-way ANOVA followed by Bonferroni post-test ($n = 3$).

2.5. Therapeutic Effects of Targeted and Combination Small Interfering RNA-Lipid Nanoparticles in Advanced Orthotopic Model of Ovarian Cancer

Individual siRNA or pooled siRNA loaded HA modified LNPs were administered intraperitoneally on day 15, 20, 25, and 30 post tumor cell inoculation at 1 mg kg^{-1} total siRNA dose (**Figure 5**). All the mice in control and NC5-tNP treatment group died by day 66 (Figure 5A,B). Average median survival of mice treated with eIF3c-tNP was 64 days and PLK1-tNP was 68.5 days. As shown in Figure 5C, the median survival of 52.5 days indicating the aggressiveness of ovarian cancer. While only 10% and 20% of mice survived in the eIF3c-tNP and PLK1-tNP groups respectively, a higher proportion of 60% mice survived in combination siRNA treatment (eP-tNP) group. We achieved an improved therapeutic benefit at eightfold lower siRNA doses (1 mg kg^{-1}) compared to previous siRNA-mediated therapeutics in an ovarian cancer model.[25,26] Additionally, it is important to notice that the individual siRNA amounts in eP-tNPs are half of the amounts represented in individual LNPs.

We also evaluated functional activity of siRNAs in combination treatment. Tumor mice were administered eP-tNPs intraperitoneally. After 48 h, ascites, ovary, and omentum were collected and analyzed for gene expression levels. We observed

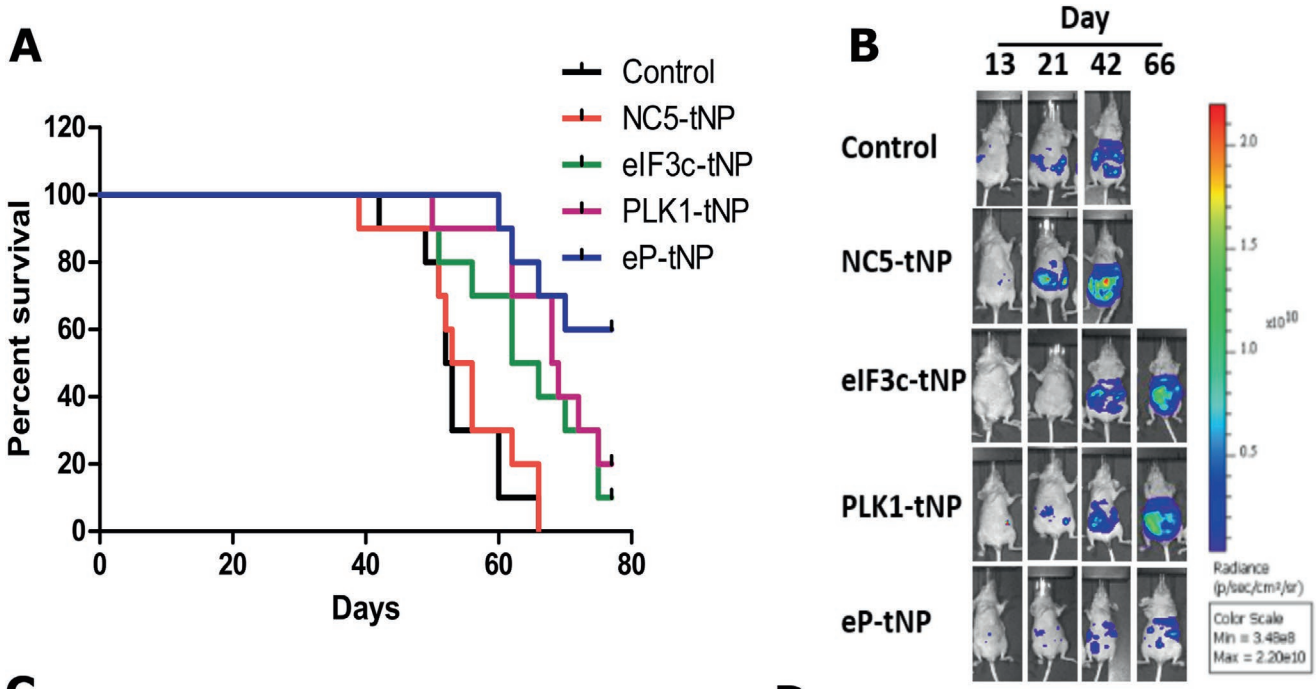

C

Group	N	Survival %	Median survival (d)	P-value
Control	10	0	52.5	
NC5-tNP	10	0	54.5	0.53 ns
eIF3c-tNP	10	10	64	0.01 (*)
PLK1-tNP	10	20	68.5	0.0003 (***)
eP-tNP	10	60	-	<0.0001 (***)

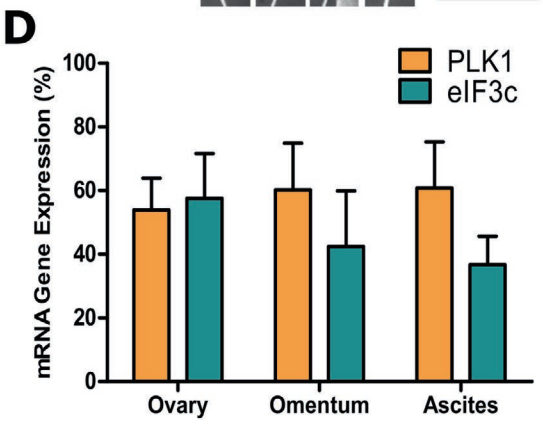

Figure 5. Nude female mice were injected IP with 3×10^6 Ovcar8 cells labelled with Luciferase. The tumors were monitored for luminescent signal to monitor tumor growth in vivo. Injections of HA-coated LNPs were administered IP on day 15, 20, 25, and 30 post tumor inoculation. A) Kaplan Meier survival graph ($n = 10$, repeated twice); B) Images of mice (Luc) from representative groups; C) Table summarizing number of animals in each group, survival (%) on last day (82) of in vivo study and median survival in days; D) HA-coated eP-LNPs were injected IP in tumor bearing mice on day 52. 48 h post-injection mice were euthanized and ovary, omentum, and ascites were harvested to extract RNA and evaluate expression (%) of target genes-PLK1 and eIF3C. GAPDH was used as endogenous control and the results are normalized to NC5-NP treatment group. Robust silencing of both genes was observed with combination siRNAs (***$p < 0.001$; two-way ANOVA followed by Bonferroni's test) ($n = 3$–5).

robust and reproducible in vivo gene silencing (between ≈40% and 60%) of both target genes—eIF3c and PLK1 (Figure 5D). Overall, these results suggest that local intraperitoneal administration of LNPs and targeting separate pathways contributing in tumor progression would be an advantage to treat aggressive peritoneal metastasis.

3. Discussion

Ovarian cancer is the leading cause of gynaecological mortality often diagnosed at advanced stage of the disease. Ovarian cancer is an aggressive tumor, which metastasizes from stage II onward to omentum, peritoneal wall, gastrointestinal tract and forms ascites in peritoneal cavity. Chemotherapy and surgical intervention are currently available treatments for ovarian cancer with toxic side effects. However, recent developments in nucleic acid-based therapies such as RNAi emerged for the treatment of various cancer types by targeting multiple signaling pathways necessary for cancer cell survival. Due to specific physiological challenges, RNAi requires suitable vehicle for delivery. Non-viral gene therapy is most advanced delivery platform for nucleic acid delivery to different cell types. Here, we devised LNP system containing lipid 10, previously shown as efficient RNAi delivery to lymphocytes with no major toxicity and adverse immune activation.[20] LNPs encapsulated siRNA were synthesized by microfluidic mixing device (Figure 1A). Physicochemical characterization of LNPs confirmed smaller

size with uniform distribution (Figure 1B–D). LNPs were further modified with hyaluronic acid (HA), a natural ligand for CD44 receptor to enhance cancer cell specific uptake and internalization specifically in tumors with reduced vascularization such as ovarian cancers.[14] The membrane glycoprotein CD44 is a known cancer stem cell (CSC) marker,[27,28] widely expressed in various tumors including breast, pancreatic, brain and ovarian cancers.[29] LNP surface altered and surface potential decreased after HA-coating (Figure 1C,E).[20] The efficiency and cellular uptake of lipid 10-LNPs were superior to MC3-LNPs (Figures S3 and S4, Supporting Information) at lower siRNA amounts. Additionally, no significant difference observed between lipid 10 and MC3 at higher doses could be due to the saturation of RISC molecules at certain RNAi amounts.[30] These results suggested that lipid 10-LNPs are efficient at lower doses that can further minimize any side effects Only at lowest concentration of siRNA equivalent, results in a clear advantage of lipid 10 in comparison to MC3. This implies that a lower dose of lipid 10 LNPs is sufficient to achieve therapeutic benefit. We also observed increased cellular uptake of lipid10-LNPs compared to MC3-LNPs in Ovcar8 cells (Figure S4, Supporting Information).[31]

In ovarian cancer, spheroid formation presents stage II or onward when cluster of tumor cells shed to metastasize in organs of peritoneal cavity and also lead to the formation of ascites in patients. Spheroids are cluster of multicellular layers making it difficult for drugs or nanoparticles to penetrate unto the innermost layer due to secretion of extracellular matrix proteins (Collagen I, Lumican, Fibronectin I) acting as physical barrier. To mimic tumor cells in cancer patients, we evaluated siRNA-LNPs efficiency on 3D cell cultures.

Spheroids have shown to be rich in CSCs and consequently it is difficult to kill the core quiescent cells. We observed very high expression of CD44 (≈1500-fold) in 3D-cultured spheroids as compared to 2D cultures (Figure 2B). Taking the advantage of CD44 overexpression, we first investigated the effect of HA coated tLNPs encapsulating both sieIF3c and siPLK1 (eP-tNP) on spheroids. A robust and efficient silencing of ≈80% of both eIF3c and PLK1 genes confirmed penetration and functional advantage of using LNP-mediated siRNA delivery (Figure 2F).

Our targeted LNP system not only inhibit the targeted genes but translated to a significant reduction in spheroid growth kinetics and volume in all HA-coated NPs (Figure 2D,E) as compared to their uncoated counterparts demonstrating that HA is crucial in LNP binding and uptake by the cells within the spheroid. This phenomenon observed previously, that Hyaluronan-Cisplatin conjugated nanoparticles attenuated the growth of 3D spheroids of Lewis lung carcinoma than with Cisplatin as free drug. This subsequently led to significant reduction in lung cancer growth in mice.[32]

Bhise et al, reported 57% transfection efficiency in 2D but only 6% in 3D cell cultures by polymeric nanoparticles with terminal modifications to facilitate transfection.[33] Brock et al utilized lipidoid nanoparticles to silence HoxA1 in cultured human mouse mammary tumor spheroids.[34] They showed a DNA synthesis reduction of ≈50% in M6 cells treated with siHoxA1 which resulted in acinar lumen formation and reduced tumor cell proliferation.

To the best of our knowledge, our eP-tNP showed the most achieved silencing ≈80% of both target genes) in 3D spheroid-based culture ever reported without modifying the growing conditions of spheroid culture.[35] Overall, the results strongly suggest that the LNPs are efficient in delivering genes in to spheroids. Additionally, HA modification on the surface of LNPs would be advantageous in tumor penetration via CD44 receptors besides targeting multiple signaling pathway by dual siRNAs in controlling spheroid growth for better therapeutic outcome.

First, the efficiency and functional activity of LNPs encapsulated with either sieIF3c or/and siPLK1 evaluated in Ovcar8 cells. The gene eIF3c forms core subunit of eIF3c complex which plays essential role in eukaryotic translation initiation. As shown in Figure 3A, a robust >90% silencing of the eIF3c genes in Ovcar8 cells treated with eIF3c-tNPs. In order to ascertain the effect of functional activity of eIF3c on protein synthesis, we performed puromycin labelling assay. Puromycin is a natural antibiotic that leads to irreversible inhibition of protein translation.[36] This is achieved by incorporating puromycin in the growing polypeptide chain, which immediately terminates translation. These newly translated puromycylated peptides can be detected using anti-Puromycin antibody.[22] We observed fainter bands in both 2D and 3D groups in eIF3c-tNP treated group (Figure 3B,C) as compared to control group which demonstrated an overall reduction in global protein synthesis.

PLK1 gene plays role in cell cycle regulation and is essential for cancer cell proliferation. Downregulation of PLK1 induced gene silencing after treatment with PLK1-tNP (Figure 3D) led to arrest of over 80% cells in the G2/M phase in cell cycle (Figure 3E,F). This further translated into apoptosis and death of over 60% cells as observed by the Annexin/PI staining (Figure 3G). Additionally, LNPs encapsulated both siPLK1 and sieIF3c (eP-tNP) efficiently downregulated both genes up to 90% at half of the siRNA dose used for individual LNPs. These observations establish the functional activity of eP-tNPs in suppressing protein synthesis essential for maintaining cellular function and cell cycle arrest. These results suggest an advantage of targeting multiple pathways by LNPs loaded with pooled siRNAs over individual LNP-siRNA system in cancer therapy.

Epithelial ovarian cancer (EOC) is the most lethal gynaecological malignancy of which high-grade serous (HGS) carcinoma represents 90% cases.[37] Interestingly, association between cellular and molecular features of 39 ovarian cancer cell lines with clinical features showed that the three most widely used cell lines—SKOV3, IGROV1, and A2780 are not the major HGS subtype.[38] Consequently, it is crucial to select relevant cell lines for in vivo model which are consistent with clinical phenotypes. In this work, we used Ovcar8 derived orthotopic tumor model which has been previously reported to belong to EOC subtype and is one of the few cells forming ascites in mice.[2] This was central to this work as a tumor model representing the heterogeneity observed across ovarian cancer patients in the clinic.

Unlike most solid tumors, ovarian cancer disseminates from stage II onward along the transcoelomic route and grows around organs of peritoneal cavity.[39] We used mCherry labelled Ovcar8 cells for evaluating therapeutic potential of LNPs. To demonstrate the nanoparticle binding to cancer cells in vivo, we labelled the LNPs with Cy5 and injected intraperitoneally in tumor bearing mice around day 48–52 when ascites is formed

(Figure 4A–C)). Besides whole mice imaging, we harvested key organs involved in ovarian cancer pathophysiology- ovary, omentum and ascites for imaging and quantifying Cy5 labelling per mCherry-tumor signal. Omentum is a well-established site for primary metastasis in cancers of colon, stomach and ovary and leads to further disease spread around peritoneal cavity.[40] In case of EOC omentectomy is performed in clinical setting to prevent local recurrence and estimating the stage of tumor. Since the binding of HA-coated NPs was significant in comparison to uNPs in ovary, omentum, and ascites (Figure 4C,D), we further confirmed our observations by evaluating in vivo silencing effect achieved with siPLK1 encapsulated tNPs. PLK1 gene expression in the ovary, omentum and ascitic fluid was significantly reduced showing robust in vivo knockdown of PLK1 gene in HA-coated treatment group as compared to uncoated uNPs. Thus, demonstrating functional advantage of using hyaluronan for targeting CD44 receptors in ovarian cancer cells.

Recent clinical trials on stage III ovarian cancer patients with primary peritoneal carcinoma compared intravenous (IV) versus intraperitoneal (IP) injection of standard chemotherapy (paclitaxel plus cisplatin).[41] Surprisingly, the median survival in IP administration group significantly improved (23.8 days) compared to IV administration (18.3 days), respectively, thereby concluding an improved survival in IP-therapy patients with optimally debulked stage III ovarian cancer. Also, in a recent work, Mills et al[42] found significant intracellular signaling of NPs in the tumor cells after IP administration compared to IV administration. Due to superiority of localized delivery of therapy in peritoneally spread tumor, we evaluated the therapeutic benefit of our nanoparticle system via IP administration. We administered first NP dose on day 15 (after injecting tumor cells) when the tumors were implanted in omentum and ovary in order to correlate late-stage clinical presentation of 80% patients (stage III and IV) with advanced peritoneal metastasis. A 60% survival of mice in the combination treatment group (eP-tNP) over single siRNA treatment clearly shows an advantage of targeting two cancer-driving pathways (Figure 5A) in minimizing cancer-associated mortality in ovarian cancer. In this study, we used 1 mg kg^{-1} LNPs injected IP which is safe and comparable to studies in existing literature.[43] CD44-specific HA-coated LNPs were mostly accumulated in tumor regions of peritoneal cavity, omentum, and ovary (Figure 4). However, we did not observe LNP accumulation in the liver and spleen suggesting that there was no significant organ toxicity at this stage due to IP administration.

Backed by aforementioned clinical trials and from our current work, we also suggest that IP administration would be advantageous in delivering siRNA therapeutics to the intended localized region of tumors and reduce systemic side effects, if any. We also demonstrate that reduced siRNA dose is sufficient for better therapeutic outcome with CD44 specific HA-LNPs, which may contribute to an improvement in the disease burden and consequent mortality from EOC in clinical setting.

4. Conclusion

Here we developed LNP system containing novel ionizable lipid to encapsulate multiple siRNAs to target multiple pathways of cancer cell survival. LNPs further surface modified with HA to target ovarian cancer cells specifically. Furthermore, intraperitoneal administration of combination siRNA-LNPs in xenografted mice bearing an orthotopic ovarian metastasis model showed robust gene silencing in target tumor bearing tissues in vivo and significantly enhanced the survival of mice compared to untreated and single siRNA loaded LNPs. These results demonstrate that intraperitoneal administration of combination eP-tLNPs could be advantageous in treating advanced peritoneal metastasis, which represents most of the clinical stages of ovarian cancer diagnoses. Further future clinical evaluation of HA-LNPs on large animals could become a promising tool to treat patients with aggressive and advanced ovarian cancer.

5. Experimental Section

Cell Culture: Ovcar8 and NAR cell lines were cultured in RPMI-1640 media supplemented with 10% fetal bovine serum, 1% penicillin/streptomycin and 2 mM L-glutamine (Biological Industries). Cells were incubated at 37 °C with 5% CO_2 and were subcultured twice per week. Ovcar8 cells were stably transfected cells using the pLL-CMV-mCherry lentivirus. Transfected cells were sorted according to their mCherry expression, and the highest mCherry population was collected.

Preparation of Lipid-Based Nanoparticles: The lipid Dlin-MC3-DMA was synthesized according to the previously reported procedure.[44] The lipid 10 was synthesized according to the procedure reported recently by our group (Figure S1, Supporting Information).[20] LNPs were prepared using microfluidic mixing procedure (Precision NanoSystems, Vancouver, BC).[8] Briefly, one volume of ethanol containing lipid mixture (ionizable lipid, DSPC, Cholesterol, DMG-PEG and DSPE-PEG-Amine at 50:10:38:1.5:0.5 mol ratio) and three volumes of desired siRNA (1:16 w/w siRNA to lipid) in acetate buffer were mixed through the micromixer at a combined flow rate of 12 mL min^{-1}. The resultant LNP solution was dialyzed against PBS (pH 7.4 using a 12–14 kDa cut-off membrane) for 16 h to remove ethanol completely. NC5 (scrambled siRNA), eIF3c, PLK1, and combination of eIF3c and PLK1 were incorporated as siRNA to form NC5-NP, eIF3c-NP, PLK1-NP, eP-NP, respectively. Non-HA coated LNPs were prepared by replacing DSPE-PEG-amine with DSPE-PEG-OMe in the lipid mix.

Functionalization of Lipid Nanoparticles with Hyaluronic Acid: HA modification of LNPs was achieved by amine coupling.[8] First carboxylic groups of HA (MW 200 kDa, Lifecore Biomedical LLC, Chaska, MN) were activated by EDC/sulpho-NHS method. HA (5×10^{-5} mmol) was dissolved in water followed by the addition of EDC (5×10^{-6} mmol) and sulfo-NHS (5×10^{-6} mmol). The reaction mixture was stirred by a gentle shaker for 1 h followed by addition of amine-functionalized nanoparticles at pH 7.8 (equivalent of (0.03 mg of PEG-amine, 1×10^{5} mmol) and stirring continued for another 2 h. The reaction mixture was dialyzed against PBS (pH 7.4 and using a 1000 kDa cut-off membrane for 24 h to remove excess HA and EDC.

Size Distribution and Zeta Potential Measurements: Particle size distribution and zeta (ζ) potential measurements were conducted before and after HA functionalization was determined by light scattering using a Malvern nano ZS ζsizer (Malvern Instruments, Ltd., Worcestershire, UK). Size measurements were performed in filtered PBS, pH 7.4, and ζ potential measurements were performed in filtered DDW. Each experimental result was an average of at least 3 independent formulations.

Ultrastructure Analysis of Hyaluronan-Lipid Nanoparticles by Electron Microscopy: The ultrastructure of HA-LNPs was investigated using transmission electron microscope (TEM). Samples were adsorbed on Formvar/carbon-coated grids and negatively stained with 2% aqueous uranyl acetate. The analysis and imaging were carried out using Jeol 1400 Plus transmission electron microscopy (Japan). Images were captured using SIS Megaview III and iTEM the TEM imaging platform (Olympus).

40μM mesh to remove clumps, RBCs were removed by hypotonic lysis in sterile MiliQ H_2O and Percoll gradient (90%/ 45%) was used to enrich the suspension with tumor cells.

Functional Activity of Eukaryotic Translation-Initiation Factor 3c by Puromycin Labelling of Newly-Synthesized Proteins: To grow cells in 3D culture, culture plates were pre-coated under sterile conditions as follows—1.2% poly-2-hydroxyethyl methacrylate (polyHEMA; Sigma Aldrich) solution in 95% ethanol was prepared. 0.75 mL of polyHEMA solution was added per well of 6-well plate which were then dried at 37 °C for 24 h before seeding cells. 0.2×10^6 Ovcar8 cells were seeded per well on a 6-well plate for 2D- and polyHEMA coated plate for 3D-culture. After 24 h cells were transfected with NC5- and eIF3c-tLNPs at 37 nM siRNA equivalent concentration and left untouched. Puromycin labelling was performed according to Aviner et al with modifications.[22] After 72 h newly synthesized proteins were labeled by 2.5 µg mL^{-1} puromycin (ThermoFisher) treatment for 5 min. Cells were washed with PBS and harvested in lysis buffer (RIPA Buffer (Merck) containing Protease Inhibitor cocktail). Total protein content was estimated using Micro BCA kit (Thermo Scientific). 200 µg mL^{-1} equivalent protein lysate in 6X loading dye with β-mercaptoethanol was boiled at 95 °C for 5 min. Samples were loaded on a 10% SDS-PAGE, transferred to a nitrocellulose membrane, and immunoblotted with anti-puromycin antibody (1:5000; clone 12D10, Milipore MABE343).

Cell Cycle Analysis: Ovcar8 cells were plated at a density of 0.1×10^6 cells in 6-well plate. After overnight adherence, cells were treated with NC5- and PLK1-tNPs (37 nM equivalent). After 24 h, cells were harvested, washed with PBS and fixed in cold 70% ethanol for 30 min at 4 °C. Cells were washed twice in PBS, spun at 850 g. RNase and propidium iodide (PI; Sigma, St. Louis, MO, USA) were added to samples. Fluorescence was measured by flow cytometry. The percentage of cells in each stage of cell cycle was determined by counting at least 10^4 cells (CytoFLEX, Beckman Coulter) and data were analyzed using CytExpert Software.

In Vitro Apoptosis Activity of Polo-like Kinase-1-Nanoparticles: Ovcar8 cells were plated at a density of 0.1×10^6 cells in 6-well plate. After overnight adherence, cells were treated with NC5- and PLK1-tNPs (37 nM equivalent). After 48 h, cells were trypsinized, washed with PBS, and labelled with annexin V-FITC and propidium iodide (PI). Apoptosis was evaluated by flow cytometer and data were analyzed using CytExpert Software.

Cellular Internalization by Confocal Microscopy: Ovcar8 cells were plated at a density of 4×10^4 cells in 12-well plate. After overnight adherence, cells were incubated with Cy5-labelled LNPs formulated with either MC3 or lipid 10 for 4 h. For the evaluation of Cy5-labelled uncoated versus HA-coated LNPs 37 nM equivalent formulation was used. Cells were washed with PBS twice and fixed with 4% paraformaldehyde for 30 min at room temperature. Cells were washed twice with PBS and blocked with BSA (2%) for 1 h at room temperature. Cells were washed and incubated with WGA-488 (1:500) for 1 h followed by nuclear staining with DAPI. Imaging was performed using a Leica SP5 confocal microscope. For quantification of the foci, intensity of staining in red channel was measured by ImageJ software. For each treatment, 50 cells (3–4 images) were analyzed, and average fluorescence intensity was plotted.

Cell Viability Assay: Ovcar8 and NAR cells were plated onto a 96-well plate at a density of 2000 cells $well^{-1}$ and incubated for 24 h (37 °C; 5% CO2). The cells were then transfected with siRNA loaded HA-tLNPs—Negative control—NC5 (NC5-tNP), eIF3c (eIF3-tNP), PLK1 (PLK1-tNP), and eP-tNP (half concentration of eIF3c and PLK1) at 7, 18, 37, and 74 nM equivalent siRNA concentrations for 3, 4, and 7 days. Cell viability was assessed by 2,3-Bis-(2-methoxy-4-nitro-5-sulfophenyl)-2H-tetrazolium-5-carboxanilide salt (XTT) assay (Cell Proliferation Kit, Biological Industries, Israel). 50 µL of reaction mixture was added per well after each time point and incubated for another 2 h. The plate is gently shaken to dissolve the orange- formazan crystals and measurements and calculations were performed as recommended by the manufacturer.

Quantification of mRNA Levels by qPCR: The mRNA levels of PLK1 and eIF3c gene in cells was quantified by real- time PCR 72 h post-transfection. Total RNA was isolated using the EzRNA purification kit (Biological industries, Israel). 1 µg RNA from each sample was reverse transcribed into cDNA using cDNA reverse transcription kit (Quanta Biosciences). Quantification of cDNA (5 ng total) was performed on the step one sequence detection system (Applied Biosystems, Foster City, CA) using Sybr green (Applied Biosystems, Foster City, CA). GAPDH was used as a housekeeping gene.

For real time PCR the following primers were chosen:
GAPDH forward: ATTCCACCCATGGCAAATTC
GAPDH reverse: GGATCTCGCTCCTGGAAGATG
eIF3c forward: ACCAAGAGAGTTGTCCGCAGTG
eIF3c reverse: TCATGGCATTACGGATGGTCC
PLK1 forward: ACCAGCACGTCGTAGGATTC
PLK1 reverse: CAAGCACAATTTGCCGTAGG

Spheroids Growth Kinetics Following Lipid Nanoparticle Treatment: Spheroids were formed by plating 2000 Ovcar8 cells in 200 µL media per well of clear round bottom ultra-low attachment 96-well plates (Corning) and kept untouched to form spheroids. After 96 h the spheroids were monitored using live cell imaging device Incucyte Zoom System (Essen Bioscience) every day until day 12 to obtain spheroid growth kinetics. A total of three consecutive treatments (LNPs with 148 nM equivalent siRNA concentration) were given starting from day 0 at the time of seeding cells and on day 4 and 8. Media was carefully refreshed from the side of each well every alternate day starting from day 4. The quantitative data was obtained from the mean red fluorescence intensity of each spheroid per well per time point. Spheroids which were found to be out focus at any time point were excluded from the data set.

Efficacy of Lipid Nanoparticles on Mice Orthotopic Model of Ovarian Cancer: Athymic nude female mice (6 weeks old) were purchased from Envigo (Israel). Mice were maintained and treated according to National Institutes of Health guidelines. All animal protocols were approved by the Tel-Aviv Institutional Animal Care and Use Committee. Mice were inoculated with 3×10^6 Luc-labelled Ovcar8 cells IP.[23] Saline was injected to mice in control group. LNPs were administered 4 times on day 15, 20, 25, 30 with 1 mg kg^{-1} mice body weight. Mice were monitored for body mass change every 3–4 days and the tumor growth in vivo was followed up by measuring luminescence signal using in vivo imaging system every week. 5 min before imaging mice were IP injected with 200 µL luciferin (60 mg kg^{-1}, Perkin Elmer) followed by isofluorane induced anaesthesia. Images were obtained with a binning factor of 8 (medium) and f stop = 2. Mice were sacrificed at the onset of ascites.

Biodistribution of Cy5-labelled Lipid Nanoparticles: Female nu/nu mice were inoculated with 3×10^6 mCherry-labelled Ovcar8 cells IP. Biodistribution studies were performed in tumor bearing mice 48–55 day post-tumor inoculation. Mice were injected with 1 mg kg^{-1} Cy5-labelled LNPs (uncoated or HA-coated) intraperitoneally and sacrificed 2 h after LNP injection. Whole mice and tumor bearing organs were harvested and imaged with CRI maestro for Cy5 and mCherry signal. For quantification of the foci, intensity of staining of both Cy5 and mCherry signals in ovary and omentum from each mice was measured by ImageJ software. For each treatment, 3–5 mice were analyzed, and average fluorescence intensity of Cy5 per unit mCherry signal was plotted.

Statistical Analysis: Statistical analysis was performed with the use of GraphPad Prism 5.03 software (GraphPad Software, San Diego, CA, USA). The results are presented as mean ± SD. More than two groups were analyzed using two-way ANOVA followed by Bonferroni post-test.

Supporting Information

Supporting Information is available from the Wiley Online Library or from the author.

Acknowledgements

The authors thank Dr. Andrea Atzmon and Dr. Orna Elroy Stein for technical assistance with Puromycin incorporation assay. This work was supported in part by the Israel Science Foundation (ISF) grant #1178/16, the Rivkin Foundation, and Len and Susan Mark Program in Ovarian Cancer awarded to D.P.

Conflict of Interest

D.P. receives licensing fees (to patents on which he was an inventor) from, invested in, consults (or on scientific advisory boards or boards of directors) for, lectured (and received a fee) or conducts sponsored research at TAU for the following entities: Alnylam Pharmaceuticals Inc. Arix Biosciences Inc., ART Biosciences, BioNtech RNA pharmaceuticals; Centricus, Diagnostear Ltd., EPM Inc., Earli Inc., Impetis Biosciences, Kernal Biologics, GPCR Inc., Medison Pharma Ltd., Newphase Ltd, NLC Pharma Ltd., Nanocell Therapeutics, NanoGhosts Ltd., Precision Nanosystems Inc., Paul Hastings Inc., Regulon, Roche, SciCann, Shire Inc., VLX Ventures, TATA Cooperation, Teva Pharmaceuticals Inc., Wize Pharma Ltd. All other authors declare no competing financial interests. S.R. receives licensing fees from BioNtech RNA pharmaceuticals. The rest of the authors declare no conflict of interest.

Data Availability Statement

The data that support the findings of this study are available from the corresponding author upon reasonable request.

Keywords

gene delivery, lipid nanoparticle, ovarian cancer, small interfering RNA, targeting

Received: January 16, 2021
Revised: February 22, 2021
Published online:

[1] R. L. Siegel, K. D. Miller, A. Jemal, *Ca-Cancer J. Clin.* **2020**, *70*, 7.
[2] E. Kipps, D. S. Tan, S. B. Kaye, *Nat. Rev. Cancer* **2013**, *13*, 273.
[3] A. J. Cortez, P. Tudrej, K. A. Kujawa, K. M. Lisowska, *Cancer Chemother. Pharmacol.* **2018**, *81*, 17.
[4] D. Rosenblum, N. Joshi, W. Tao, J. M. Karp, D. Peer, *Nat. Commun.* **2018**, *9*, 1410.
[5] C. Liang, J. Chang, Y. Jiang, J. Liu, L. Mao, M. Wang, *Chem. Commun.* **2019**, *55*, 8170.
[6] M. S. Singh, D. Peer, *Curr. Opin. Biotechnol.* **2016**, *39*, 28.
[7] H. Wood, *Nat. Rev. Neurol.* **2018**, *14*, 570.
[8] Z. R. Cohen, S. Ramishetti, N. Peshes-Yaloz, M. Goldsmith, A. Wohl, Z. Zibly, D. Peer, *ACS Nano* **2015**, *9*, 1581.
[9] E. M. Smekalova, M. V. Gerashchenko, P. B. F. O'Connor, C. A. Whittaker, K. J. Kauffman, A. S. Fefilova, T. S. Zatsepin, R. L. Bogorad, P. V. Baranov, R. Langer, V. N. Gladyshev, D. G. Anderson, V. Koteliansky, *Mol. Ther.– Nucleic Acids* **2020**, *19*, 252.
[10] R. Emmanuel, S. Weinstein, D. Landesman-Milo, D. Peer, *Cancer Lett.* **2013**, *336*, 158.
[11] W. Zhao, X. Li, J. Wang, C. Wang, Y. Jia, S. Yuan, Y. Huang, Y. Shi, Z. Tong, *Med. Sci. Monit.* **2017**, *23*, 4182.
[12] H. Y. Lee, C. K. Chen, C. M. Ho, S. S. Lee, C. Y. Chang, K. J. Chen, Y. S. Jou, *Oncotarget* **2018**, *9*, 13193.
[13] J. Hao, Z. Wang, Y. Wang, Z. Liang, X. Zhang, Z. Zhao, B. Jiao, *Oncol. Rep.* **2015**, *33*, 2954.
[14] J. I. Hare, T. Lammers, M. B. Ashford, S. Puri, G. Storm, S. T. Barry, *Adv. Drug Delivery Rev.* **2017**, *108*, 25.
[15] A. B. Alvero, R. Chen, H. H. Fu, M. Montagna, P. E. Schwartz, T. Rutherford, D. A. Silasi, K. D. Steffensen, M. Waldstrom, I. Visintin, G. Mor, *Cell Cycle* **2009**, *8*, 158.
[16] S. Zhang, C. Balch, M. W. Chan, H. C. Lai, D. Matei, J. M. Schilder, P. S. Yan, T. H. Huang, K. P. Nephew, *Cancer Res.* **2008**, *68*, 4311.
[17] K. Y. Choi, H. Y. Yoon, J. H. Kim, S. M. Bae, R. W. Park, Y. M. Kang, I. S. Kim, I. C. Kwon, K. Choi, S. Y. Jeong, K. Kim, J. H. Park, *ACS Nano* **2011**, *5*, 8591.
[18] K. Cohen, R. Emmanuel, E. Kisin-Finfer, D. Shabat, D. Peer, *ACS Nano* **2014**, *8*, 2183.
[19] N. N. Parayath, A. Parikh, M. M. Amiji, *Nano Lett.* **2018**, *18*, 3571.
[20] S. Ramishetti, I. Hazan-Halevy, R. Palakuri, S. Chatterjee, S. N. Gonna, N. Dammes, I. Freilich, L. K. Shmuel, D. Danino, D. Peer, *Adv. Mater.* **2020**, *32*, 1906128.
[21] M. S. Singh, M. Goldsmith, K. Thakur, S. Chatterjee, D. Landesman-Milo, T. Levy, L. A. Kunz-Schughart, Y. Barenholz, D. Peer, *Nanoscale* **2020**, *12*, 1894.
[22] R. Aviner, S. Hofmann, T. Elman, A. Shenoy, T. Geiger, R. Elkon, M. Ehrlich, O. Elroy-Stein, *Nucleic Acids Res.* **2017**, *45*, 5945.
[23] D. Rosenblum, A. Gutkin, R. Kedmi, S. Ramishetti, N. Veiga, A. M. Jacobi, M. S. Schubert, D. Friedmann-Morvinski, Z. R. Cohen, M. A. Behlke, J. Lieberman, D. Peer, *Sci. Adv.* **2020**, *6*, eabc9450.
[24] A. K. Mitra, D. A. Davis, S. Tomar, L. Roy, H. Gurler, J. Xie, D. D. Lantvit, H. Cardenas, F. Fang, Y. Liu, E. Loughran, J. Yang, M. S. Stack, R. E. Emerson, K. D. C. Dahl, M. V. B. , K. P. Nephew, D. Matei, J. E. Burdette, *Gynecol. Oncol.* **2015**, *138*, 372.
[25] D. Polyak, A. Krivitsky, A. Scomparin, S. Eliyahu, H. Kalinski, S. Avkin-Nachum, R. Satchi-Fainaro, *J. Controlled Release* **2017**, *257*, 132.
[26] N. Jyotsana, A. Sharma, A. Chaturvedi, R. Budida, M. Scherr, F. Kuchenbauer, R. Lindner, F. Noyan, K. W. Suhs, M. Stangel, D. Grote-Koska, K. Brand, H. P. Vornlocher, M. Eder, F. Thol, A. Ganser, R. K. Humphries, E. Ramsay, P. Cullis, M. Heuser, *Ann. Hematol.* **2019**, *98*, 1905.
[27] R. Bhattacharya, T. Mitra, S. R. Chaudhuri, S. S. Roy, *J. Cell. Biochem.* **2018**, *119*, 3373.
[28] R. Thapa, G. D. Wilson, *Stem Cells Int.* **2016**, *2016*, 2087204.
[29] J. Zhou, Y. Du, Y. Lu, B. Luan, C. Xu, Y. Yu, H. Zhao, *Front. Oncol.* **2019**, *9*, 802.
[30] G. Cuccato, A. Polynikis, V. Siciliano, M. Graziano, M. di Bernardo, D. di Bernardo, *BMC Syst. Biol.* **2011**, *5*, 19.
[31] A. S. Nunes, A. S. Barros, E. C. Costa, A. F. Moreira, I. J. Correia, *Biotechnol. Bioeng.* **2019**, *116*, 206.
[32] S. Ishiguro, S. Cai, D. Uppalapati, K. Turner, T. Zhang, W. C. Forrest, M. L. Forrest, M. Tamura, *Pharm. Res.* **2016**, *33*, 2517.
[33] N. S. Bhise, R. S. Gray, J. C. Sunshine, S. Htet, A. J. Ewald, J. J. Green, *Biomaterials* **2010**, *31*, 8088.
[34] A. Brock, S. Krause, H. Li, M. Kowalski, M. S. Goldberg, J. J. Collins, D. E. Ingber, *Sci. Transl. Med.* **2014**, *6*, 217ra2.
[35] R. G. Morgan, A. C. Chambers, D. N. Legge, S. J. Coles, A. Greenhough, A. C. Williams, *Sci. Rep.* **2018**, *8*, 7952.
[36] R. Aviner, *Comput. Struct. Biotechnol. J.* **2020**, *18*, 1074.
[37] D. D. Bowtell, S. Bohm, A. A. Ahmed, P. J. Aspuria, R. C. Bast Jr., V. Beral, J. S. Berek, M. J. Birrer, S. Blagden, M. A. Bookman, J. D. Brenton, K. B. Chiappinelli, F. C. Martins, G. Coukos, R. Drapkin, R. Edmondson, C. Fotopoulou, H. Gabra, J. Galon, C. Gourley, V. Heong, D. G. Huntsman, M. Iwanicki, B. Y. Karlan, A. Kaye, E. Lengyel, D. A. Levine, K. H. Lu, I. A. McNeish, U. Menon, S. A. Narod, B. H. Nelson, K. P. Nephew, P. Pharoah, D. J. Powell Jr., *Nat. Rev. Cancer* **2015**, *15*, 668.
[38] C. M. Beaufort, J. C. Helmijr, A. M. Piskorz, M. Hoogstraat, K. Ruigrok-Ritstier, N. Besselink, M. Murtaza, I. W. F. van, A. A. Heine, M. Smid, M. J. Koudijs, J. D. Brenton, E. M. Berns, J. Helleman, *PLoS One* **2014**, *9*, e103988.
[39] D. S. Tan, R. Agarwal, S. B. Kaye, *Lancet Oncol.* **2006**, *7*, 925.
[40] D. Collins, A. M. Hogan, D. O'Shea, D. C. Winter, *J. Gastrointest. Surg.* **2009**, *13*, 1138.
[41] D. K. Armstrong, B. Bundy, L. Wenzel, H. Q. Huang, R. Baergen, S. Lele, L. J. Copeland, J. L. Walker, R. A. Burger, *N. Engl. J. Med.* **2006**, *354*, 34.

[42] K. A. Mills, J. M. Quinn, S. T. Roach, M. Palisoul, M. Nguyen, H. Noia, L. Guo, J. Fazal, D. G. Mutch, S. A. Wickline, H. Pan, K. C. Fuh, *Sci. Rep.* **2019**, *9*, 4762.

[43] J. E. Dahlman, C. Barnes, O. Khan, A. Thiriot, S. Jhunjunwala, T. E. Shaw, Y. Xing, H. B. Sager, G. Sahay, L. Speciner, A. Bader, R. L. Bogorad, H. Yin, T. Racie, Y. Dong, S. Jiang, D. Seedorf, A. Dave, K. S. Sandu, M. J. Webber, T. Novobrantseva, V. M. Ruda, A. K. R. Lytton-Jean, C. G. Levins, B. Kalish, D. K. Mudge, M. Perez, L. Abezgauz, P. Dutta, L. Smith, K. Charisse, M. W Kieran, K. Fitzgerald, M. Nahrendorf, D. Danino, R. M Tuder, U. H von Andrian, A. Akinc, A. Schroeder, D. Panigrahy, V. Kotelianski, R. Langer, D. G Anderson, *Nat. Nanotechnol.* **2014**, *9*, 648.

[44] M. Jayaraman, S. M. Ansell, B. L. Mui, Y. K. Tam, J. Chen, X. Du, D. Butler, L. Eltepu, S. Matsuda, J. K. Narayanannair, K. G. Rajeev, I. M. Hafez, A. Akinc, M. A. Maier, M. A. Tracy, P. R. Cullis, T. D. Madden, M. Manoharan, M. J. Hope, *Angew. Chem.* **2012**, *51*, 8529.